Designing sensitive and selective polymer/enzyme composite biosensors for brain monitoring *in vivo*

Robert D. O'Neill, John P. Lowry, Gaia Rocchitta, Colm P. McMahon, Pier A. Serra

Amperometric polymer/enzyme composite (PEC) biosensors, incorporating a poly(o-phenylenediamine) ultra-thin permselective barrier, possess a variety of characteristics that make them suitable for monitoring brain energy and neurotransmitter dynamics *in vivo*. This review highlights PEC sensitivity and selectivity parameters, which allow development of the basic design in a systematic way in order to improve their performance and to diversify the analyte range of these novel probes of brain function.

Keywords: Ascorbic acid interference; Brain monitoring; Electropolymerization; Glucose; Glutamate; H_2O_2 permeability; Polymer-modified electrode

Robert D. O'Neill*, Gaia Rocchitta[1], Colm P. McMahon, Pier A. Serra[1]
UCD School of Chemistry and Chemical Biology, University College Dublin, Belfield, Dublin 4, Ireland

John P. Lowry
Department of Chemistry, National University of Ireland, Maynooth, Co. Kildare, Ireland

*Corresponding author.
Tel.: +353 1 7162314;
Fax: +353 1 7161178;
E-mail: Robert.ONeill@UCD.ie

[1]Present address: Department of Pharmacology, Medical School, University of Sassari, Viale S. Pietro 43/b, 07100, Sassari, Italy.

1. Introduction

Understanding the mechanisms underlying the functioning of the human brain stands at the forefront of modern science. Behavior, feelings, thoughts and even consciousness itself may reflect the interplay of its electrical and chemical pathways. Clinical intervention in neurological disorders is usually achieved using chemical agents that act on neuromediator-related sites, suggesting that intercellular chemical signaling plays a major role in determining the properties of neural networks. However, measuring real-time chemical events in the living brain is a supreme technical challenge, even in animal models, and involves many biocompatibility issues. A growing number of analytical methodologies are being developed, including sampling [1,2], spectroscopic [3] and electrochemical [4–6], to study neurochemical dynamics in the intact brain. One such set of techniques involves the *in-situ* detection of substances in brain extracellular fluid (ECF) using implanted biosensors.

Electrochemical biosensors exploit the specificity of a biological component, usually an enzyme immobilized on the electrode [7–10], to provide sensitivity to a target analyte. The chemical specificity can be very high, even to the level of stereoselectivity (e.g., the use of L-glutamate oxidase (GluOx) in the design of amperometric biosensors to detect neurotransmitter L-glutamate [11,12]).

However, the remarkable specificity of enzyme-based amperometric biosensors can be seriously undermined by interference from electroactive species present in the target medium, compromising the selectivity of the device. This problem is particularly pronounced for biosensors implanted in biological tissues for real-time monitoring [9,10,13,14], because separation techniques cannot be exploited to eliminate the interference, as is the case for on-line microdialysis approaches to *in-vivo* monitoring [8,15–17]. Despite this drawback, considerable efforts have been made over the past two decades to overcome issues of *in-vivo* biosensor sensitivity, selectivity and stability, mainly because of the significant benefits of biosensor monitoring: small probe size, minimizing tissue damage [18–20]; and high time resolution, allowing real-time correlation with animal behavior [8,10,13,21].

0165-9936/$ - see front matter © 2007 Elsevier Ltd. All rights reserved. doi:10.1016/j.trac.2007.11.008

2. Designs of biosensors for brain implantation

Biosensors are powerful analytical tools whose range of applications in medical diagnostics [22], food-quality control [23] and environmental monitoring [24] is rapidly expanding. The design of an electrochemical biosensor is predicated first on the target analyte and the choice of appropriate biological element (e.g., L-glutamate detection has been achieved using either glutamate receptor ion channels [22], glutamate oxidase [25] or glutamate dehydrogenase [26], and the respective electrochemical steps can be very different [22]).

However, the vast majority of enzyme-based amperometric biosensors exploit the biocatalytic oxidation of analyte, using oxidase enzymes containing the prosthetic group, flavin adenine dinucleotide (FAD). Despite this common foundation, a wide range of oxidase-based devices have been designed to make use of different signal-transduction mechanisms and diverse selectivity strategies [7,9,10,22,26–29].

Another key factor shaping biosensor design is the nature of the intended application matrix [10,24] (e.g., devices for monitoring analyte-concentration dynamics *in vivo* must be biocompatible over the time course of the implantation, both in terms of tissue effects on sensor functionality, and physiological reaction to the probe [20,30,31]). As well as possessing the appropriate level of biocompatibility, implantable oxidase-based biosensors must also fulfill the following minimum criteria for reliable analyte monitoring:

- appropriate size and geometry [32,33];
- good sensitivity to the enzyme substrate [34];
- effective rejection of electroactive interference [35,36]; and,
- low sensitivity to changes in pO_2 over the range of substrate and oxygen concentrations relevant to the intended application [11,37].

Even different tissues present distinct challenges. For example, biosensors designed to monitor glucose in blood or subcutaneous fat *in vivo* need a significantly greater oxygen tolerance compared to devices for monitoring brain ECF [38], because glucose levels are an order of magnitude higher in these peripheral tissues than in brain ECF [39].

Within these restrictions, a number of biosensor designs have been developed and applied to monitor concentration dynamics of specific brain analytes *in vivo*. Among the first to be reported were those based on organic conducting salt tetrathiafulvalene tetracyanoquinodimethane (TTF-TCNQ) [40,41]. Although initially thought to involve direct electron transfer between the FAD center and this novel conducting surface, there is now evidence that signal generation is mediated by TCNQ° from the electrode material [42,43]. It is interesting to note that one of these seminal studies applied the concept of a 'blank' sensor (one containing all the design elements of the biosensor, but omitting the enzyme) implanted beside the biosensor in order to minimize electroactive interference, using subtraction. This strategy was necessary because interference by ascorbic acid (AA, archetypal electroactive species that contaminates biosensor signals *in vivo*) can occur even at the low anodic potentials used for this class of biosensor [40,44]. The use of blank sensors coupled with biosensors in difference mode is now seen as a vital component of reliable brain monitoring [33,35,45–50], although the use of a blank sensor does not mitigate the problem of oxygen dependence of oxidase-generated signals.

A more common design of biosensor used for analysis of brain systems (including brain slices *in vitro* and intact tissue *in vivo*) incorporates redox hydrogels (e.g., osmium poly(vinyl pyridine) redox polymer [51–53]), and this biosensor design has also been implanted in peripheral tissues [54]. The Os-gel-HRP provides mediated electron transfer between the horseradish peroxidase, which reacts with the H_2O_2 generated according to Reactions 1 and 2, and the electrode operating at mild cathodic applied potentials [35]. These devices may also include ascorbic acid oxidase and Nafion to reduce further interference by AA.

Neurochemical studies *in vivo*, using these probes, have been limited to acute implantation in anesthetized preparations, and it is unclear at present whether this class of biosensor is stable enough to allow long-term brain monitoring in freely-behaving animals. The presence of anesthetic is an important issue for *in-vivo* monitoring studies because different, and sometimes opposite, effects on neurochemical dynamics have been observed in the presence of anesthesia [10]. Thus, for example, it is unwise to test the glutamate/ascorbate heteroexchange hypothesis in chloral hydrate anesthetized rats, using this class of biosensor [50], when it has been demonstrated explicitly that chloral hydrate blocks this exchange [55].

A design, which has recently been implanted successfully for chronic recording in the brain of unanesthetized animals, exploits the anion-rejecting properties of Nafion as the main strategy for reducing electroactive interference at a ceramic-based biosensor [4,56], in addition to a blank or 'sentinel' electrode to increase further the selectivity of the detection system [33,49]. The biosensor signal is generated by direct oxidation of H_2O_2 on the electrode surface (Reactions 1–3) at a relatively high applied anodic potential. Studies carried out over seven days showed that there was little loss of the sensitivity of the implanted differential device [33], which indicates a promising future for this approach. However, an issue that needs to be addressed before widespread applications are undertaken is the oxygen dependence of these biosensors, which has yet to be reported. A variation on this design, which incorporates additional polymer layers deposited over a platinum

substrate, has been applied for acute recording of brain glucose [57], lactate [58] and glutamate [48].

The use of poly-*ortho*-phenylenediamine (PPD) as a permselective membrane in the fabrication of implantable sensors and biosensors has been reported by a number of laboratories [59–64]. Indeed, PPD has been used in the construction of biosensors for a range analytes in different target media [63,65–71]. PPD can be deposited electrochemically from *o*-phenylenediamine (*o*PD) solutions at neutral pH to produce a thin, self-sealing, insulating polymer on the electrode surface [69]. Film-thickness estimations for PPD generated under these conditions are typically in the region of 10–30 nm [69,72–74]. As well as possessing excellent interference-rejection characteristics, PPD also serves as a method of immobilizing enzymes and protects the electrode surface from fouling [39,70], making it ideal for biosensor applications *in vivo* [10]. The signal in this design is also generated by the direct oxidation of H_2O_2 on the electrode surface (Reactions 1–3) at relatively high applied anodic potentials. A main advantage of PPD-based glucose biosensors is their stability, even during amperometric recording over days in freely behaving animals [39,63,75,76]. In addition, the pO_2 dependence of both glucose- [38,63] and glutamate- [11,32,77] detecting forms of these biosensors has been quantified in detail, and shown to be adequate for brain monitoring (see Section 6 below). Thus, although each design of biosensor for brain monitoring has a key advantage, such as the small cross-section of Os/gel/HRP-based carbon-fiber electrodes [53,78] and the self-referencing capability of the ceramic-based devices [49], the overall long-term stability and oxygen tolerance of PPD-based biosensors make them an attractive choice for further development [11,65,79–82].

Here, we review the design of biosensors based on PPD polymer/enzyme composite (PEC) permselective layers for *in-vivo* neurochemical monitoring, with particular emphasis on the usefulness of biosensor sensitivity and selectivity parameters.

3. PEC-biosensor notation

To allow functionality in the electrochemically hostile environment of living brain tissue, implantable biosensors often contain a variety of components to enhance their sensitivity, selectivity and stability. These agents are laid down in an order that depends on their intended role, and so, in defining a systematic notation, this order must be clear. The nomenclature employed here uses a slash to indicate consecutive layering from left to right,

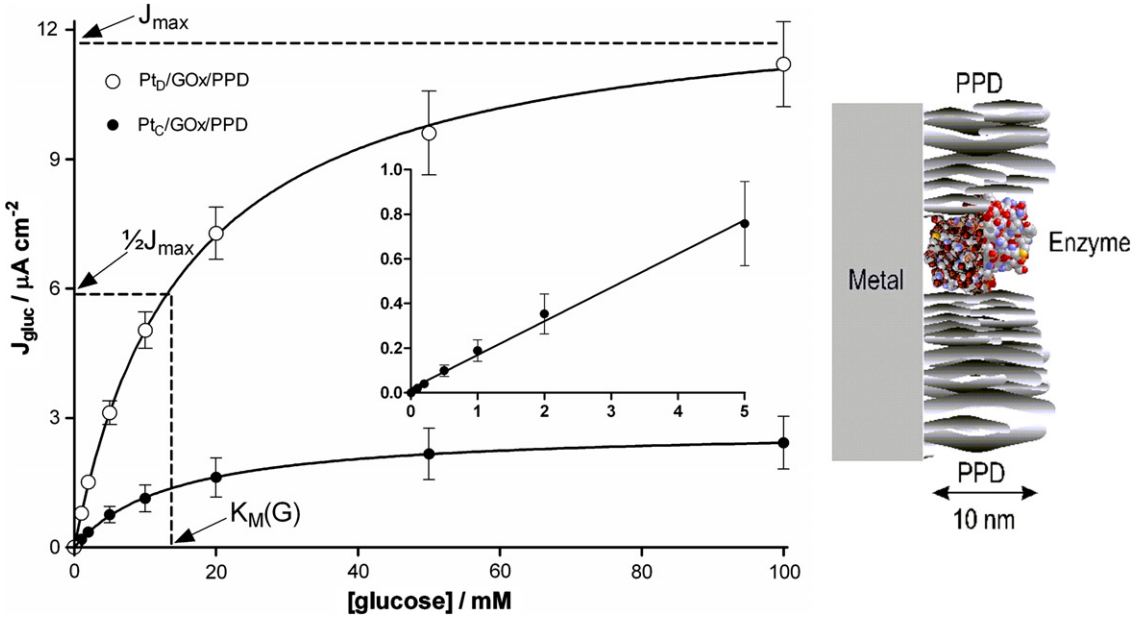

Figure 1. The effects of electrode geometry on the glucose response of GOx/PPD-based biosensors, illustrated by glucose calibrations performed using cylinder (C, •) and disk (D, o) based devices of the type where the GOx was adsorbed on the Pt before electropolymerization of PPD (see schematic on the right). Points are means ± SEM of current densities; curves were generated using non-linear regression and Equation (7a) ($R^2 > 0.99$). The enzyme loading density (Equation 11) is much greater for the disk biosensors due to more efficient dip-evaporation enzyme deposition compared with cylinders [38]. However, the mean apparent K_M value for glucose, $K_M(G)$, was not significantly different for these two designs: 15 ± 2 mM ($n = 21$); 15 ± 1 mM ($n = 4$); $p > 0.94$ [38]. ***Inset:*** Part of the linear region glucose response (Equation 10) for the Pt_C/GOx/PPD configuration, showing the regression line with $R^2 = 0.995$ and using the same axis units as the main graph. Plots and schematic are adapted from [38].

while components deposited simultaneously are separated by a hyphen. For example: Pt/GOx/PPD represents glucose oxidase (GOx) deposited on Pt (normally by dip evaporation [77,83]) followed by electropolymerization of PPD (see Fig. 1); Pt/PPD/GOx indicates GOx deposited over electropolymerized PPD; and Pt/GOx-PPD signifies the co-deposition of enzyme and polymer by including GOx in the monomer solution. This notation is quite flexible and, where necessary, allows for such details as: the geometry of the electrode (e.g., disks (D) or cylinders (C) that can significantly affect biosensor performance [11,77,84] (see Fig. 1)); the number of dip coatings applied (four in the following example); and, the stock-solution concentration of the agent deposited (e.g., 200 U/mL): Pt_D/GOx(200U)$_4$/PPD.

4. Enzyme-related biosensor parameters

A number of sophisticated mathematical models of the behavior of enzymes in membranes have been described [85,86]. These complex analyses are often needed to understand and to optimize the behavior of thick and/or conducting layers [87]. However, a recent study has shown that substrate diffusion is not limiting for PPD layers incorporating enzymes [88], due to their ultra-thin nature (10-30 nm [69,72,74]). The basic Michaelis-Menten enzyme parameters used here therefore provide more readily accessible insights into factors affecting the responsiveness of biosensors fabricated from the insulating form of PPD, and avoid the use of more complex analyses, such as those involving the Thiele modulus [89].

For oxidase enzyme (E) with FAD as prosthetic group, the catalytic conversion of substrate (S) and co-substrate (O_2) to products (P) and H_2O_2 can be written as Reactions (1)–(3):

$$S + E/FAD \rightarrow P + E/FADH_2 \quad (1)$$

$$E/FADH_2 + O_2 \rightarrow E/FAD + H_2O_2 \quad (2)$$

$$H_2O_2 \rightarrow O_2 + 2H^+ + 2e^- \quad (3)$$

The two-substrate form of the Michaelis-Menten equation for the overall rate of reaction, v, is given by Equation (4) [89,90]:

$$v = \frac{v_{max}}{1 + K_M(S)/[S] + K_M(O_2)/[O_2]} \quad (4)$$

If the concentration of the co-substrate is large and constant, Equation (4) reduces to:

$$v = \frac{v'_{max}}{1 + K_M(S)/[S]} \quad (5)$$

Equation (5) represents the rate of product formation, which in this case reflects the rate of H_2O_2 generation. The H_2O_2 generated in the enzyme layer is the species detected at the electrode surface, but its bulk concentration is zero; it is the flux of H_2O_2 from the immobilized enzyme to the conducting surface that determines the current. Converting the rate (Equation (5)) to current (Equation (6)) is achieved by multiplying both sides by A$\alpha z\boldsymbol{F}$, where α is the fraction of the flux that is oxidized on the electrode of geometric area, A (some H_2O_2 is lost to the bulk [76]). Consistent with this analysis, many biosensor designs respond hyperbolically to the bulk concentration of enzyme substrate, and v'_{max} (Equation (5)) is related to I_{max} (Equation (6)) through the A$\alpha z\boldsymbol{F}$ term. The value of K_M, the concentration of substrate that yields $v_{max}/2$, does not change with this conversion. When comparing biosensors of different sizes, the response (I_S) can be normalized to current density (J_S, Equation (7a)) by dividing by area, A. Nonlinear regression analysis of J_S *vs.* [S] provides the basic response parameters: J_{max}, K_M(S) and R^2. Alternatively, if the concentration of S is fixed and O_2 levels are changed, then Equation (7b) can be used to analyze the oxygen dependence of the signal [32,63], where J'_{max} is the maximum (plateau) response for a particular concentration of S, and $K_M(O_2)$ is the apparent Michaelis constant for oxygen.

$$I_S = \frac{I_{max}}{1 + K_M(S)/[S]} \quad (6)$$

$$J_S = \frac{J_{max}}{1 + K_M(S)/[S]} \quad (7a)$$

$$J_S = \frac{J'_{max}}{1 + K_M(O_2)/[O_2]} \quad (7b)$$

The current density for the biosensor response to S, J_S, is a measure of the overall rate of the enzyme reaction, and J_{max} is the J_S value at enzyme saturation. Different values of J_{max}, determined under the same conditions, reflect differences in the activity of enzyme on the surface (k_2[E]; see Reaction (8)) [38], provided the sensitivity of the electrode to H_2O_2 (Reaction (3)) does not vary much, as is the case for many of the PPD-modified Pt cylinders and disks used in brain monitoring [10,63,76].

The Michaelis constant, K_M, is defined in terms of the rate constants for the generalized reactions (Reaction (8)) describing the conversion of substrate to products, catalyzed by the enzyme (see Equation (9)). However, when Equation (7a) is used to approximate the two-substrate case, K_M is more complex and contains co-substrate terms. K_M is then the *apparent* Michaelis constant and phenomenologically defines the concentration of substrate that gives half the J_{max} response (see Fig. 1). Thus, changes in K_M are sensitive to the binding constant, k_1, and have been interpreted in terms of barriers to substrate/enzyme binding [70,91], as well as changes in oxygen demand [11,38,77,92]. When comparing biosensor parameters based on different enzymes (e.g., GOx and GluOx (L-glutamate oxidase)), it may be necessary to specify the enzyme substrate (e.g., K_M(G) vs.

K_M(Glu)). When analyzing the influence of co-substrate (O_2) on the biosensor response, $K_M(O_2)$ and K_M(S) must be distinguished [11,77].

$$E + S \underset{k_{-1}}{\overset{k_1}{\rightleftharpoons}} ES \xrightarrow{k_2} E + P \quad (8)$$

$$K_M = \frac{k_{-1} + k_2}{k_1} \quad (9)$$

The apparent Michaelis constant for S is also useful for defining the range of linear response to S (up to $\sim 1/2K_M$), as well as the slope in the linear region (LRS), that is, LRS $\approx J_{max}/K_M$; see Equation (10).

$$Lt_{[S]\to 0} J_S = \frac{J_{max}}{1 + K_M/[S]} = \frac{J_{max}[S]}{[S] + K_M} \approx \frac{J_{max}}{K_M}[S] \quad (10)$$

Biosensors are usually designed to operate in real applications within their linear region response to analyte, which is generally considered to extend as far as $K_M/2$. For biosensors incorporating GluOx, intended to detect low levels of Glu in biological samples, a critical property is high sensitivity in the linear region, whereas the range of linearity in not a problem. Since LRS $\approx J_{max}/K_M$ (Equation (10)), increasing enzyme loading is a common strategy in the quest for increased LRS. However, the plot of LRS versus J_{max} in Fig. 2 shows that the experimentally measured LRS does not increase with J_{max} for Pt_D/GluOx/PPD biosensors because there is a corresponding increase in K_M(Glu) for this design due to electrostatic repulsion between the anionic Glu analyte and the high polyanionic enzyme density on these disk surfaces [84]. Neutralization of this repulsion by incorporating polycationic polyethyleneimine (PEI) into the PEC matrix restored this valuable correlation (Fig. 2), allowing significant increases in LRS values [11].

The turnover of O_2 in PEC membranes (Reaction (2)) depends on the rate at which substrate binds to the enzyme (Reaction (1)) (i.e. on substrate concentration). Glucose is an example of an analyte with relatively high concentrations in brain ECF, so it is a useful model system for quantifying PEC sensitivity to changes in ECF pO_2. Experiments over a range of glucose concentrations, including 0.5, 2.5 and 10.0 mM glucose, were performed *in vitro*, where the pO_2 was controlled in a sealed environment, and the Pt/GluOx/PPD signal monitored as a function of dissolved oxygen concentration [38,63] (see Fig. 3). The smaller the value of $K_M(O_2)$ in Equation (7b), the lower the oxygen dependence because higher oxygen affinity leads to oxygen saturation at lower pO_2, thereby reducing biosensor dependency at higher pO_2 levels. As predicted, O_2 dependence became more acute at higher glucose concentrations. For 10-mM glucose, a level not much greater than the normoglycemic value in human blood [93] and less than that observed under hyperglycemic diabetic conditions [94], the O_2 dependence was close to maximal (near-linear biosensor response to pO_2) with a $K_m(O_2) = \sim 150$ μM [38]. The Pt/PPD/GOx sensor design would therefore not be suitable for monitoring blood glucose *in vivo*. Fig. 3 also shows the glucose-O_2 correlation plot for 0.5-mM glucose; the plot was hyperbolic, consistent with Equation (7b), with $R^2 > 0.997$, and values of $K_m(O_2)$ in the range 5–10 μM. The 0.5-mM glucose current therefore displayed a low insensitivity to changes in O_2 levels at average brain ECF levels of O_2 (~40 μM O_2). These *in-vitro* results suggest that Pt/PPD/GOx electrodes might be suitable for brain monitoring, where the estimated glucose level is much lower than that in blood. Indeed, ECF glucose has been determined to be an order of magnitude lower than blood levels by both quantitative microdialysis (350 ± 16 μM [39]) and biosensor studies (300–400 μM [95]) in the striatum of the awake rat. We discuss the experimental oxygen dependence of PEC-based biosensors *in vivo* in Section 6 below.

When the biosensor incorporates a component that significantly affects the sensitivity of the surface to H_2O_2 (e.g., Nafion or lipid phosphatidylethanolamine (PEA)), then variations in J_{max} across sensor populations may be due to changes in either enzyme activity or H_2O_2

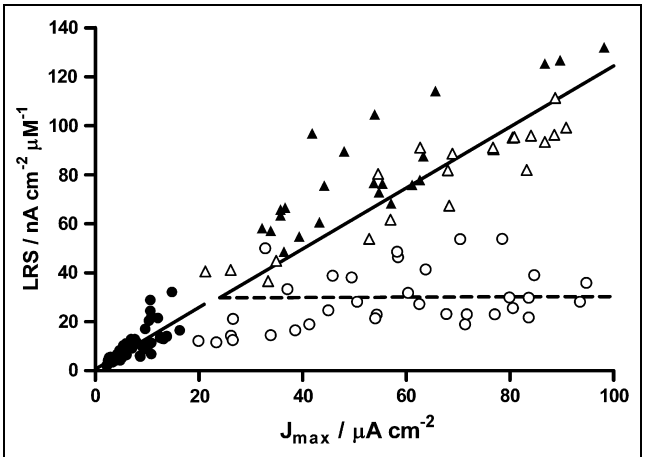

Figure 2. Example of the effects of J_{max} and K_M on the linear region slope (LRS). J_{max} was varied by controlling enzyme loading, and J_{max}, K_M and the LRS measured experimentally (see Fig. 1) in the presence and absence of polycationic polyethyleneimine (PEI) in the PEC layer. Section of the scatter plots and linear regression analyses for the Glu calibration linear region slope (LRS) *versus* J_{max} (Equation 10) for four biosensor designs fabricated by depositing the polymer/enzyme composite GluOx/PPD on either Pt_C (filled circles, $n = 55$), Pt_D (open circles, $n = 61$), Pt_C/PEI (filled triangles, $n = 27$) or Pt_D/PEI (open triangles, $n = 20$). On bare Pt at low GluOx loading (small J_{max}), i.e., for Pt_C-based biosensors, there is a systematic increase in LRS with J_{max} (slope = 1.3 ± 0.2, $R^2 = 0.54$, $p < 0.0001$, $n = 55$). On bare Pt at higher GluOx loading, i.e., for the Pt_D-based devices, there is no change in LRS with J_{max} (slope = 0.01 ± 0.02, $R^2 = 0.003$, $p > 0.65$, $n = 61$). When PEI was incorporated into the PEC layer, there was a systematic increase in LRS with J_{max} for both cylinders and disks (combined slope = 1.2 ± 0.1, $R^2 = 0.49$, $p < 0.0001$, $n = 47$). Thus, PEI led to convergence of the responses for the two geometries. Plots and analysis are adapted from [11].

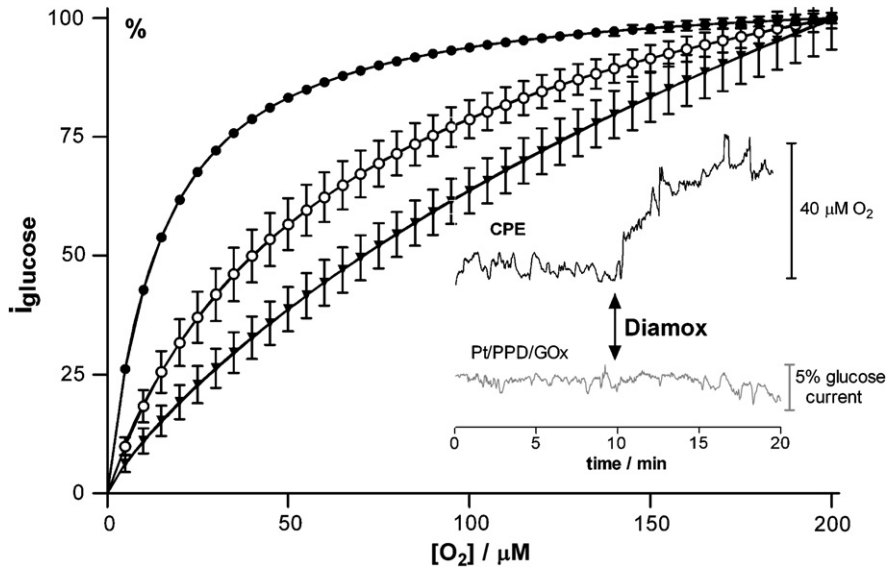

Figure 3. Increase in oxygen dependence at higher concentrations of substrate for Pt/GOx/PPD biosensors *in vitro*. Examples of averaged normalized glucose-oxygen correlation plots for three concentrations of glucose (filled circle, 0.5 mM, $n = 3$; open circle, 2.5 mM, $n = 7$; triangle, 10 mM, $n = 6$) studied over the relevant range of O_2 concentration (N_2 saturation to air saturation) showing the increased sensitivity of the biosensor signal to solution pO_2 as the concentration of glucose is increased [38,63]. The non-linear regression plots shown were obtained using Equation (7b). ***Inset***. The effect of systemic administration of the carbonic anhydrase inhibitor (Diamox, 50 mg/kg, i.p.) on the O_2 and glucose signals monitored simultaneously *in vivo* in rat brain striatum. Comparison of the O_2 current (black, recorded using DPA with a carbon paste electrode, CPE, in the left striatum) and glucose signal (grey, detected using amperometry at +700 mV with a Pt/GOx-PPD electrode in the right striatum) illustrates that O_2 availability does not impact significantly on glucose monitoring in brain ECF *in vivo*, where baseline glucose levels are in the region of 0.5 mM [39]. Plots are adapted from [63].

sensitivity. The activity of surface enzyme itself depends on two factors: the density of active enzyme molecules on the surface (active enzyme loading, [E]); and, the value of the catalytic rate constant, k_2 (Reaction (8)). Thus, enzyme activity is k_2[E], and these two terms are rarely separable, especially for implantable microelectrodes where dip evaporation is used to deposit enzyme on the biosensor surface (i.e. [E] is not known independently). A useful approximation to the effective activity of surface enzyme is the parameter $[E]_{act}$, defined in Equation (11), where slope(HP) is the calibration slope for H_2O_2 at the biosensor. Certainly, variations in $[E]_{act}$ determined under the same conditions will reflect changes in k_2[E], which in turn often arise from changes in [E] [84].

$$[E]_{act} = \frac{J_{\max}}{slope(HP)} \tag{11}$$

$$\mathrm{BE\%} = \frac{slope(\mathrm{S}) * 100\%}{slope(HP)} \tag{11a}$$

An analogous, and possibly more useful, parameter, which also normalizes the biosensor response with respect to H_2O_2 sensitivity, is biosensor efficiency (BE%) (see Equation (11a), where slope(S) is the LRS for enzyme substrate). In theory, the absolute maximum value of BE% should be 100% if the surface is saturated with enzyme, all the H_2O_2 produced by the enzyme is electrooxidized on the surface, and the diffusion coefficients of S (D_S) and H_2O_2 are equal. Since D_S will always be less than that for H_2O_2 ($\sim 1.0 \times 10^{-5}$ cm^2/s) and some H_2O_2 is lost to the bulk even in quiescent solution [76], then $(\mathrm{BE\%})_{\max} < 100\%$. An empirical maximum appears to be close to 60% [84], which is consistent with these factors.

Two additional parameters related to biosensor response to substrate, S, are useful. Response times can be recorded in constantly stirred solution, using a data-acquisition rate of >10 Hz [32]. A $t_{90\%}$ parameter has been defined as the time taken for the analyte response to reach 90% of its maximum value from the start (<10%) of the current upswing, and is similar to definitions used elsewhere [4,50,96]. The limit of detection (LOD) of S is usually determined using the widely applied criterion of three times the SD of the baseline. Response time and LOD are particularly crucial when designing biosensors to monitor fast transients in brain neurotransmitters whose ECF levels are invariably low (e.g., L-glutamate, Glu). PEC-based devices (e.g., Pt/GluOx/PPD) show good behavior in these respects, with $t_{90\%}$ values of ~3 s (just 1 s slower than to bulk H_2O_2) and an LOD of <0.5 µM Glu [32,83].

5. Polymer-related biosensor parameters

The main analytical parameters of the surface polymer are related to

(i) the sensitivity of the sensor to the target analyte and the electroactive enzyme-transducer molecule (H_2O_2; Reactions (1)–(3)); and,
(ii) its ability to reject interference species, especially ascorbic acid (AA).

The starting point for determining these properties is the sensitivity to H_2O_2 and AA at the bare metal. First, the current-density responses of AA at bare microdisks and cylinders are the same, as are those of H_2O_2, indicating that subtle differences in diffusion profiles are not significant in this context [65,97]. A direct comparison of the amperometric sensitivity of pure Pt and Pt-Ir has also been carried out [65,98]. A small loss of H_2O_2 sensitivity for the alloy compared with the pure metal was observed, presumably due to the involvement of Pt oxides in H_2O_2 electro-oxidation. The greater sensitivity of both bare metal-electrode types for H_2O_2 compared with AA is in line with diffusion-coefficient values for the two analytes and diffusion-limited kinetics at the operational applied potential (700 mV vs. SCE) [65].

$$2H_2O_2 \rightarrow 2H_2O + O_2 \qquad (12)$$

Using a large population of wire electrodes, the hypothesis that ultra-thin (10–30 nm [69,72,74]) electrosynthesized PPD does not decrease the sensitivity of Pt-Ir to H_2O_2 has been tested [65]. Surprising, the large sample size revealed that PPD-modified Pt-Ir showed a small, but statistically significant, increase in the H_2O_2 calibration slope (189 ± 10 μA/cm^2/mM, n = 51) compared with the bare metal (171 ± 6 μA/cm^2/mM, n = 51, p = 0.05 for a paired t-test). One possible explanation for the unexpected small increase in the efficiency of the electrochemical H_2O_2 oxidation on the coated metal is that PPD inhibits the H_2O_2 disproportionation reaction (Reaction (12)) at the electrode surface, the extent of which varies with electrode condition. However, it is clear that the basic Pt-Ir/PPD design displays near-optimal H_2O_2 sensitivity, so that the only effective way to improve selectivity significantly is to increase interference blocking by the polymer layer. The more robust Pt-Ir working electrodes are therefore generally used for implantable biosensors *in vivo*, and normally designated as Pt for simplicity of notation. The permeability of the PEC layer to H_2O_2 can therefore be defined as in Equation (13), and is normally about 100 ± 10% for the basic Pt/Ox/PPD designs [65,97,99].

$$\mathrm{P(HP)\%} = \frac{slope(HP)\ at\ Pt/PEC * 100\%}{slope(HP)\ at\ Pt} \qquad (13)$$

An unusual property of PPD-based PEC layers is their ability to reject AA more efficiently at higher AA concentrations (Fig. 4). Indeed, at extremely low levels of AA, the response of Pt/PPD electrodes is similar to bare Pt; however, even at 10-μM AA, AA sensitivity (I_{AA}/[AA]) is considerably lower than that at bare metal [99]. AA, and/or its oxidation product, trapped in the polymer matrix therefore appears to cooperate efficiently with PPD in a form of ''self blocking'' [74,99], so that, by concentrations in the 100-μM region, the AA response is essentially flat (Fig. 4). Because of this non-linear behavior of AA at Pt/PEC electrodes, the 1-mM value (plateau response, I_{lim}; see Fig. 4) is used in the corresponding definition of AA permeability, P(AA)% (Equation (14)).

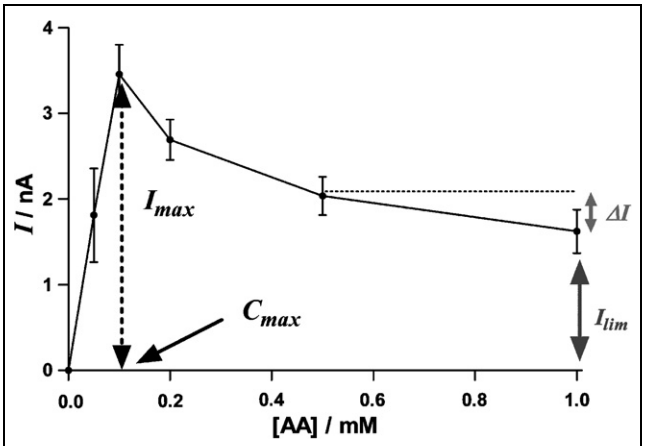

Figure 4. The calibration profile obtained by plotting steady-state responses *vs.* AA concentration for Pt/PPD electrodes. Because of the non-linearity of the AA response at these electrodes, it is necessary to quantify the response in a number of ways. Firstly, the maximum current response, $\boldsymbol{I}_{max}$ and the concentration at which $\boldsymbol{I}_{max}$ occurs, $\boldsymbol{C}_{max}$. This parameter gives a good indication of the appropriate application of the sensors; for example, AA is present in tissues at concentrations ranging from 50 μM in blood to 500 μM in brain ECF. Thirdly, the current at 1 mM AA (generally the plateau region), $\boldsymbol{I}_{lim}$, which serves for comparisons of the absolute AA blocking ability of different polymers. Lastly, the current associated with the concentration change from 0.5 mM to 1 mM (i.e., equivalent to doubling brain ECF levels), $\boldsymbol{\Delta I}$, an even better indication of the interference blocking ability of the polymer in neurochemical analysis *in vivo*. Plot are adapted from [74].

$$\mathrm{P(AA)\%} = \frac{I_{lim}(AA)\ at\ Pt/PEC * 100\%}{slope(AA)\ at\ Pt} \qquad (14)$$

The main focus in using P(HP)% is to maintain its value as close to 100% as possible (see above). The finding that values of P(HP)% greater than 100% have been observed indicates that this is not a true permeability, possibly due to complications (e.g., Reaction (12)). However, P(AA)% is very small (~0.2% [65,74]) and probably reflects the poor ability of AA to permeate the PEC layer. The problems with interpreting P(HP)% indicate that the permselectivity, S_P%, defined by Equation (15), is probably not the most useful parameter for quantifying PEC selectivity.

$$S_P\% = \frac{P(AA)\% * 100\%}{P(HP)\%} \qquad (15)$$

Instead, the equimolar selectivity, S%, defined by Equation (16), is a good index of the relative sensitivities

of the PEC-coated metal to the two analytes. Because S% represents a percentage interference, the smaller the value, the more suitable the polymer is for biosensor applications, and values as low as ~0.2% have been reported for PPD-based devices [65,74].

$$S\% = \frac{I_{\lim}(AA)\ at\ Pt/PEC * 100\%}{slope(HP)\ at\ Pt/PEC} \quad (16)$$

However, the polymer composite can also affect the behavior of the trapped enzyme [38,77]. Thus, although S% is a good parameter for monitoring the effects of the polymer layer on relative H_2O_2 and AA sensitivities, and a good (low) value of S% is a prerequisite for a successful biosensor design, it is not sufficient. Having established a good S% value, it is necessary to quantify the effects of the polymer composite on enabling the production of H_2O_2 by the enzyme. The biosensor LRS for substrate is the best measure of the biosensor's analytical signal strength (see Equation (10)), incorporating both its ability to generate H_2O_2 enzymatically and its electrochemical sensitivity to this molecule. Thus, we might define the equimolar substrate selectivity, S_S%, by Equation (17), which will be intrinsically larger (worse) than S% due to factors discussed above.

$$S_S\% = \frac{I_{\lim}(AA)\ at\ Pt/PEC * 100\%}{LRS\ at\ Pt/PEC} \quad (17)$$

Finally, the substrate concentration in the ECF needs to be taken into account by defining S_S(ECF)% as Equation (18), where I_S(ECF) is the current for the estimated average baseline concentration of target analyte, S, obtained by scaling the LRS. S_S(ECF)% is a measure of the contributions of AA and S to the baseline biosensor response recorded in the ECF.

$$S_S(ECF)\% = \frac{I_{\lim}(AA)\ at\ Pt/PEC * 100\%}{I_S(ECF)\ at\ Pt/PEC} \quad (18)$$

A useful variation on S_S(ECF)% is $S_S(ECF_\Delta)$%, which is the substrate-selectivity parameter based on doubling baseline ECF levels of both S and AA (Equation (19)). The significance of ΔI(AA) can be seen in Fig. 4, and I_S(ECF) has the same value as for Equation (18). This latter parameter provides a measure of the percentage interference by AA in *changes* in the biosensor signal recorded in brain ECF, and therefore represents a key selectivity parameter for *in vivo* applications.

$$S_S(ECF_\Delta)\% = \frac{\Delta I(AA)atPt/PEC * 100\%}{I_S(ECF)atPt/PEC} \quad (19)$$

It is not so important that some of these later selectivity coefficients generate larger values than the more common standard S% parameter. More critical is the evolution of the value of the selectivity parameter of choice with systematic fine tuning of the biosensor design.

6. Brain monitoring with PEC-based biosensors *in vivo*

The high baseline levels of glucose in brain ECF (~0.5 mM [39]), coupled with the excellent permselectivity of PPD-based biosensors, have made it possible to

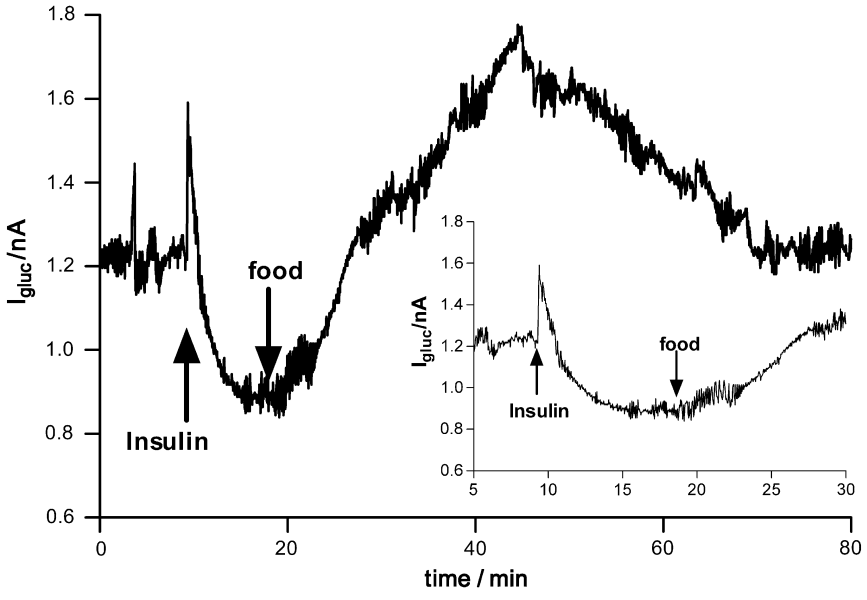

Figure 5. The response of a Pt/GOx-PPD electrode implanted in the striatum of a freely-moving fasting rat over a 80-min period, 12 days after sensor implantation. Injection of insulin (15 U/kg, i.p. – see ***Inset***) caused a decrease in the level of the signal which was reversed by the ingestion of food (see Inset) [75,76]. Plots are adapted from [76].

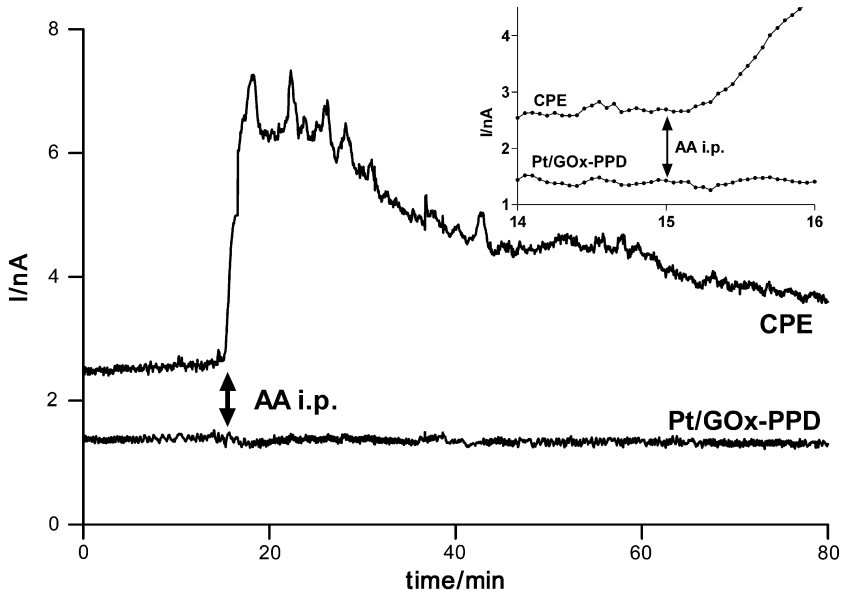

Figure 6. Effect of ascorbate injection (2 g/kg, i.p. – see ***Inset***) on the amperometric response of a carbon paste electrode (CPE) at 200 mV and a Pt/GOx-PPD electrode at 700 mV, implanted bilaterally in the striatum of the rat, 8 days after implantation. Plots are adapted from [76].

monitor physiologically and pharmacologically related concentration dynamics of this energy metabolite *in vivo* [39,61,63,75,76,100]. Many of these studies used devices of the type Pt/GOx-PPD because these can be fabricated in a one-step procedure by incorporating enzyme in the monomer solution, in contrast to the multiple dip-evaporation protocol for Pt/GOx/PPD sensors. In addition, the comparable sensitivity to glucose of these two designs has been demonstrated [83].

As outlined in Section 2, a main advantage of PPD-based glucose biosensors is their stability, even during amperometric recording over several days in freely behaving animals [39,63,75,76]. Fig. 5 shows the response of a Pt/GOx-PPD biosensor, which had been implanted in rat-brain striatum 12 days previously, to the systemic administration of insulin. The inset (Fig. 5) shows that this hormone produced a sustained depression in brain-ECF-glucose levels, which could be reversed by the ingestion of food (access to food had been restricted for the previous 12 h). The effects of insulin on brain-ECF glucose have been confirmed recently using a PPD-based biosensor incorporating a ruthenium layer [61], although the baseline observed *in vivo* with these devices was not as stable as that recorded with Ru-free PEC design (Fig. 5).

In addition to the PEC layer maintaining its sensitivity to brain glucose, the permselective membrane is also capable of rejecting AA interference after long periods implanted in the tissue. Fig. 6 shows that systemic administration of AA, at a dose that doubled brain-ECF AA levels (detected with an implanted carbon-paste electrode, CPE), had no significant effect on the Pt/GOx-PPD biosensor signal (inset, bottom). A similar combination of bilaterally implanted biosensor and CPE has been used to confirm the *in-vitro* findings (see Fig. 3) that, for physiologically relevant ECF concentrations of glucose and oxygen, oxygen demand does not limit biosensor functionality. Fig. 3 (inset) illustrates that systemic injection of a carbonic anhydrase inhibitor (Diamox), which significantly raised simultaneously monitored brain ECF pO_2, had no detectable effect on the Pt/GOx-PPD signal [63].

Taken together, the literature reports on Pt/GOx-PPD indicate that these biosensors possess sufficient glucose sensitivity, selectivity and stability to monitor this energy metabolite reliably in brain ECF over extended periods. However, the challenge remains to be how to boost PEC performance even further to allow the analogous Pt/GluOx/PPD devices to monitor brain-ECF-Glu dynamics at levels two orders of magnitude lower than those of glucose. The incorporation of polycationic PEI into the PEC design has provided an important step in that direction by enhancing the Glu sensitivity significantly (see Fig. 2). Preliminary results *in vivo* with these PEI-modified biosensors indicate that long-term Glu monitoring may soon be possible with further fine turning of this design [45].

Acknowledgements

This work was supported in part by funding from Science Foundation Ireland (03/IN3/B376 and 04/BR/C0198) and by the Health Research Board, Ireland (RP/2004/44).

References

[1] M.C. Parkin, S.E. Hopwood, D.A. Jones, P. Hashemi, H. Landolt, M. Fabricius, M. Lauritzen, M.G. Boutelle, A.J. Strong, J. Cereb. Blood Flow Metab. 25 (2005) 402.
[2] C.S. Chaurasia, M. Muller, E.D. Bashaw, E. Benfeldt, J. Bolinder, R. Bullock, P.M. Bungay, E.C.M. Delange, H. Derendorf, W.F. Elmquist, M. Hammarlund-Udenaes, C. Joukhadar, D.L. Kellogg, C.E. Lunte, C.H. Nordstrom, H. Rollema, R.J. Sawchuk, B.W.Y. Cheung, V.P. Shah, L. Stahle, U. Ungerstedt, D.F. Welty, H. Yeo, AAPS J. 9 (2007) E48.
[3] F. Crespi, A.C. Croce, S. Fiorani, B. Masala, C. Heidbreder, G. Bottiroli, Lasers Surg. Med. 34 (2004) 39.
[4] J.J. Burmeister, M. Palmer, G.A. Gerhardt, Anal. Chim. Acta 481 (2003) 65.
[5] P.E.M. Phillips, G.D. Stuber, M.L.A.V. Heien, R.M. Wightman, R.M. Carelli, Nature (London) 422 (2003) 614.
[6] R.D. O'Neill, S.C. Chang, J.P. Lowry, C.J. McNeil, Biosens. Bioelectron. 19 (2004) 1521.
[7] N. Dale, S. Hatz, F.M. Tian, E. Llaudet, Trends Biotechnol. 23 (2005) 420.
[8] M. Fillenz, Neurosci. Biobehav. Rev. 29 (2005) 949.
[9] G.S. Wilson, R. Gifford, Biosens. Bioelectron. 20 (2005) 2388.
[10] R.D. O'Neill, J.P. Lowry, M. Mas, Crit. Rev. Neurobiol. 12 (1998) 69.
[11] C.P. McMahon, G. Rocchitta, S.M. Kirwan, S.J. Killoran, P.A. Serra, J.P. Lowry, R.D. O'Neill, Biosens. Bioelectron. 22 (2007) 1466.
[12] O.M. Schuvailo, S. Gaspar, A.P. Soldatkin, E. Csoregi, Electroanalysis (N. Y.) 19 (2007) 71.
[13] J.P. Lowry, R.D. O'Neill, in: C.A. Grimes, E.C. Dickey, M.V. Pishko (Editors), Encyclopedia of Sensors, Vol. 6, American Scientific Publishers, California, USA, 2006, p. 501.
[14] P. Pantano, W.G. Kuhr, Electroanalysis (N. Y.) 7 (1995) 405.
[15] B. Fumero, T. Guadalupe, F. Valladares, F. Mora, R.D. O'Neill, M. Mas, J.L. Gonzalez-Mora, J. Neurochem. 63 (1994) 1407.
[16] X.P. Ao, J.A. Stenken, Methods 38 (2006) 331.
[17] C.J. Watson, B.J. Venton, R.T. Kennedy, Anal. Chem. 78 (2006) 1391.
[18] A. Duff, R.D. O'Neill, J. Neurochem. 62 (1994) 1496.
[19] R.D. O'Neill, J.L. Gonzalez-Mora, M.G. Boutelle, D.E. Ormonde, J.P. Lowry, A. Duff, B. Fumero, M. Fillenz, M. Mas, J. Neurochem. 57 (1991) 22.
[20] J.L. Peters, L.H. Miner, A.C. Michael, S.R. Sesack, J. Neurosci. Methods 137 (2004) 9.
[21] M. Fillenz, R.D. O'Neill, J. Physiol. (London) 374 (1986) 91.
[22] A. Hirano, M. Sugawara, Mini-Rev. Med. Chem. 6 (2006) 1091.
[23] V. Andreu, C. Blasco, Y. Pico, Trends Anal. Chem. 26 (2007) 534.
[24] S. Rodriguez-Mozaz, M.J.L. de Alda, D. Barcelo, Anal. Bioanal. Chem. 386 (2006) 1025.
[25] N. Hamdi, J.J. Wang, E. Walker, N.T. Maidment, H.G. Monbouquette, J. Electroanal. Chem. 591 (2006) 33.
[26] S. Chakraborty, C.R. Raj, Electrochem. Commun. 9 (2007) 1323.
[27] T. Ahuja, I.A. Mir, D. Kumar, Rajesh, Biomaterials 28 (2007) 791.
[28] E. Lojou, P. Bianco, J. Electroceram. 16 (2006) 79.
[29] G.S. Wilson, Y.B. Hu, Chem. Rev. 100 (2000) 2693.
[30] R.D. O'Neill, Analyst (Cambridge, U. K.) 118 (1993) 433.
[31] F. Ahmad, A. Christenson, M. Bainbridge, A.P.M. Yusof, S. Ab Ghani, Biosens. Bioelectron. 22 (2007) 1625.
[32] C.P. McMahon, R.D. O'Neill, Anal. Chem. 77 (2005) 1196.
[33] E.C. Rutherford, F. Pomerleau, P. Huettl, I. Stromberg, G.A. Gerhardt, J. Neurochem. 102 (2007) 712.
[34] H.E. Koschwanez, W.M. Reichert, Biomaterials 28 (2007) 3687.
[35] J.J. Mitala, A.C. Michael, Anal. Chim. Acta 556 (2006) 326.
[36] K. McAteer, R.D. O'Neill, Analyst (Cambridge, U. K.) 121 (1996) 773.
[37] L. Lin, J.T. Guthrie, J. Membrane Sci. 278 (2006) 173.
[38] C.P. McMahon, S.J. Killoran, R.D. O'Neill, J. Electroanal. Chem. 580 (2005) 193.
[39] J.P. Lowry, R.D. O'Neill, M.G. Boutelle, M. Fillenz, J. Neurochem. 70 (1998) 391.
[40] M.G. Boutelle, C. Stanford, M. Fillenz, W.J. Albery, P.N. Bartlett, Neurosci. Lett. 72 (1986) 283.
[41] Q. Xin, R.M. Wightman, Anal. Chim. Acta 341 (1997) 43.
[42] C.C. Jung, E.A.H. Hall, Anal. Chem. 67 (1995) 2393.
[43] D. Centonze, I. Losito, C. Malitesta, F. Palmisano, P.G. Zambonin, J. Electroanal. Chem. 435 (1997) 103.
[44] J.P. Lowry, R.D. O'Neill, J. Electroanal. Chem. 334 (1992) 183.
[45] G. Rocchitta, C.P. McMahon, P.A. Serra, S.M. Kirwan, F.B. Bolger, J.P. Lowry, R.D. O'Neill, in: G. Di Chiara, E. Carboni, V. Valentini, E. Acquas, V. Bassareo, C. Cadoni (Editors), Monitoring Molecules in Neuroscience, University of Cagliari, Cagliari, Italy, 2006, p. 331.
[46] W.H. Oldenziel, G. Dijkstra, T.I.F.H. Cremers, B.H.C. Westerink, Brain Res. 1118 (2006) 34.
[47] M.G. Garguilo, A.C. Michael, J. Neurosci. Methods 70 (1996) 73.
[48] Y. Hu, K.M. Mitchell, F.N. Albahadily, E.K. Michaelis, G.S. Wilson, Brain Res. 659 (1994) 117.
[49] J.J. Burmeister, G.A. Gerhardt, Trends Anal. Chem. 22 (2003) 498.
[50] N.V. Kulagina, L. Shankar, A.C. Michael, Anal. Chem. 71 (1999) 5093.
[51] T. Oka, C. Tasaki, H. Sezaki, M. Sugawara, Anal. Bioanal. Chem. 388 (2007) 1673.
[52] W.H. Oldenziel, G. Dijkstra, T.I.F.H. Cremers, B.H.C. Westerink, Anal. Chem. 78 (2006) 3366.
[53] N.V. Kulagina, A.C. Michael, Anal. Chem. 75 (2003) 4875.
[54] D.W. Schmidtke, A. Heller, Anal. Chem. 70 (1998) 2149.
[55] R.D. O'Neill, M. Fillenz, L. Sundstrom, J.N.P. Rawlins, Neurosci. Lett. 52 (1984) 227.
[56] J.P. Bruno, C. Gash, B. Martin, A. Zmarowski, F. Pomerleau, J. Burmeister, P. Huettl, G.A. Gerhardt, Eur. J. Neurosci. 24 (2006) 2749.
[57] Y.B. Hu, G.S. Wilson, J. Neurochem. 68 (1997) 1745.
[58] Y.B. Hu, G.S. Wilson, J. Neurochem. 69 (1997) 1484.
[59] S.B. Hocevar, M. Zivin, A. Milutinovic, M. Hawlina, E.A. Hutton, B. Ogorevc, Front. Biosci. 11 (2006) 2782.
[60] B.A. Patel, M. Arundell, K.H. Parker, M.S. Yeoman, D. O'Hare, Anal. Chem. 78 (2006) 7643.
[61] O.M. Schuvailo, O.O. Soldatkin, A. Lefebvre, R. Cespuglio, A.P. Soldatkin, Anal. Chim. Acta 573 (2006) 110.
[62] N.R. Ferreira, A. Ledo, J.G. Frade, G.A. Gerhardt, J. Laranjinha, R.M. Barbosa, Anal. Chim. Acta 535 (2005) 1.
[63] B.M. Dixon, J.P. Lowry, R.D. O'Neill, J. Neurosci. Methods 119 (2002) 135.
[64] M. Fillenz, J.P. Lowry, Exp. Physiol. 83 (1998) 233.
[65] S.M. Kirwan, G. Rocchitta, C.P. McMahon, J.D. Craig, S.J. Killoran, K.B. O'Brien, P.A. Serra, J.P. Lowry, R.D. O'Neill, Sensors 7 (2007) 420.
[66] P.N. Bartlett, D. Pletcher, J. Zeng, J. Electrochem. Soc. 144 (1997) 3705.
[67] J.M. Cooper, P.L. Foreman, A. Glidle, T.W. Ling, D.J. Pritchard, J. Electroanal. Chem. 388 (1995) 143.
[68] J. Wang, H. Wu, Anal. Chim. Acta 283 (1993) 683.
[69] C. Malitesta, F. Palmisano, L. Torsi, P.G. Zambonin, Anal. Chem. 62 (1990) 2735.
[70] S.V. Sasso, R.J. Pierce, R. Walla, A.M. Yacynych, Anal. Chem. 62 (1990) 1111.

[71] J.I. Reyes-De-Corcuera, R.P. Cavalieri, J.R. Powers, J.M. Tang, D.H. Kang, J. Agr. Food Chem. 53 (2005) 8866.
[72] S. Myler, S. Eaton, S.P.J. Higson, Anal. Chim. Acta 357 (1997) 55.
[73] Y. Ohnuki, H. Matsuda, T. Ohsaka, N. Oyama, J. Electroanal. Chem. 158 (1983) 55.
[74] J.D. Craig, R.D. O'Neill, Analyst (Cambridge, U. K.) 128 (2003) 905.
[75] J.P. Lowry, M. Miele, R.D. O'Neill, M.G. Boutelle, M. Fillenz, J. Neurosci. Methods 79 (1998) 65.
[76] J.P. Lowry, K. McAteer, S.S. El Atrash, A. Duff, R.D. O'Neill, Anal. Chem. 66 (1994) 1754.
[77] C.P. McMahon, G. Rocchitta, P.A. Serra, S.M. Kirwan, J.P. Lowry, R.D. O'Neill, Anal. Chem. 78 (2006) 2352.
[78] W.H. Oldenziel, M. van der Zeyden, G. Dijkstra, W.E.J.M. Ghijsen, H. Karst, T.I.F.H. Cremers, B.H.C. Westerink, J. Neurosci. Methods 160 (2007) 37.
[79] K.B. O'Brien, S.J. Killoran, R.D. O'Neill, J.P. Lowry, Biosens. Bioelectron. 22 (2007) 2994.
[80] G. Rocchitta, R. Migheli, S. Dedola, G. Calia, M.S. Desole, E. Miele, J.P. Lowry, R.D. O'Neill, P.A. Serra, Serra, Sens. Actuators, B 126 (2007) 700.
[81] P.A. Serra, G. Rocchitta, G. Bazzu, A. Manca, G.M. Puggioni, J.P. Lowry, R.D. O'Neill, Sens. Actuators, B 122 (2007) 118.
[82] S.J. Killoran, D.K. Rai, R.D. O'Neill, J. Neurochem. 102 (2007) 196.
[83] M.R. Ryan, J.P. Lowry, R.D. O'Neill, Analyst (Cambridge, U. K.) 122 (1997) 1419.
[84] C.P. McMahon, G. Rocchitta, P.A. Serra, S.M. Kirwan, J.P. Lowry, R.D. O'Neill, Analyst (Cambridge, U. K.) 131 (2006) 68.
[85] R. Baronas, F. Ivanauskas, F. Ivanauskas, J. Kulys, J. Math. Chem. 35 (2004) 199.
[86] P.V. Bernhardt, Aust. J. Chem. 59 (2006) 233.
[87] J.J. Gooding, E.A.H. Hall, D.B. Hibbert, Electroanalysis (N. Y.) 10 (1998) 1130.
[88] J.I.R. De Corcuera, R.P. Cavalieri, J.R. Powers, J. Electroanal. Chem. 575 (2005) 229.
[89] J.J. Gooding, E.A.H. Hall, Electroanalysis (N. Y.) 8 (1996) 407.
[90] J.K. Leypoldt, D.A. Gough, Anal. Chem. 56 (1984) 2896.
[91] D. Compagnone, G. Federici, J.V. Bannister, Electroanalysis (N. Y.) 7 (1996) 1151.
[92] Y.N. Zhang, G.S. Wilson, Anal. Chim. Acta 281 (1993) 513.
[93] J.A. Eyre, A.G. Stuart, R.J. Forsyth, D. Heaviside, K. Bartlett, Brain Res. 635 (1994) 349.
[94] R.E. Hofer, W.L. Lanier, Anesthesiology 75 (1991) 673.
[95] J.P. Lowry, M. Fillenz, Bioelectrochemistry 54 (2001) 39.
[96] M.O.M. Berners, M.G. Boutelle, M. Fillenz, Anal. Chem. 66 (1994) 2017.
[97] C.P. McMahon, S.J. Killoran, S.M. Kirwan, R.D. O'Neill, J. Chem. Soc. Chem. Commun. (2004) 2128.
[98] Y. Zhang, G.S. Wilson, J. Electroanal. Chem. 345 (1993) 253.
[99] J.P. Lowry, R.D. O'Neill, Electroanalysis (N. Y.) 6 (1994) 369.
[100] L.I. Netchiporouk, N.F. Shram, N. Jaffrezic-Renault, C. Martelet, R. Cespuglio, Anal. Chem. 68 (1996) 4358.

Robert D. O'Neill: BSc (Chemistry, University College Dublin (UCD), Ireland, 1976); Ryan Gold Medal (Chemistry, 1976); PhD (Electrochemistry, supervised by Prof. David Feakins, UCD, 1980). Postdoctoral research (1980–83) with John Albery, FRS (Chemistry, Imperial College London) and Marianne Fillenz, MD, PhD (Physiology, Oxford University). Research Fellowships (1983–85) in Physiology (Worcester College, Oxford) and Neurochemistry (Beit Memorial Fellowship in Medical Research) at Oxford University. Appointed to UCD in 1985 and is now UCD Professor of Electrochemistry. Core research interests include: design and characterization of amperometric sensors and biosensors; electrosynthesis of non-conducting polymer layers; kinetics of surface-bound enzymes; neurotransmitter glutamate and dopamine monitoring; and, brain vitamin-C/glutamate interactions.

John P. Lowry: BSc (Chemistry, University College Dublin (UCD), Ireland, 1988); PhD (Bioelectrochemistry, supervised by Prof. Robert D. O'Neill, UCD, 1992). Postdoctoral research (1992–94; 1997–98) with Prof. O'Neill, UCD. Marie Curie Fellow (1994–97) with Marianne Fillenz, MD, PhD (University Laboratory of Physiology, Oxford). Appointed as Lecturer in Analytical Chemistry, Chemistry Department, National University of Ireland, Maynooth (NUIM) in 1998. Appointed as Lecturer in Pharmacology, Pharmacology Department, Conway Institute of Biomolecular and Biomedical Research, UCD in 2004. Appointed to Chair of Chemistry and Head of Department, NUIM, in 2006, and Adjunct Professor of Pharmacology, UCD, in 2007. Core research interests include application of brain microdialysis and amperometric sensors and biosensors in real-time studies of the interaction of neurochemical systems in the living brain. This work is targeted at understanding their role in neurochemical processes (e.g., brain energy metabolism), and also in psychiatric (e.g., schizophrenia) and neurological (e.g., Parkinson's disease) dysfunctions in order to develop treatments based on new drug discovery.

Gaia Rocchitta: MSc in Chemistry. In 2004, she received her PhD in Neuroscience at Sassari University, Italy, under the direction of Prof. M.S. Desole and Prof. E. Miele and the supervision of G. Esposito. She has recently worked as a Postdoctoral Fellow at University College of Dublin. Her main research interests involve development of glutamate biosensors and their application for *in vivo* detection of glutamate in rats in physiological and pathological conditions.

Colm P. McMahon: BSc (Hons) and PhD (2005) from University College Dublin, the latter under the direction of Prof. Robert O'Neill. His thesis work revealed the influence of biosensor geometry on the permselectivity and oxygen-dependence properties of PPD-based biosensors.

Pier Andrea Serra: Professor of Pharmacology at University of Sassari, Medical School, Italy. He received his degree as Medical Doctor at Sassari University in 1998. He studied the *in vivo* neurochemistry of Parkinson's disease using microdialysis and voltammetry under the supervision of Dr. Maddalena Miele and received his PhD in Pharmacology and Toxicology from Sassari University in 2001. He worked as a Postdoctoral Fellow at University College of Dublin under the direction of Prof. Robert D. O'Neill and Dr. John P. Lowry. His main research interest involves the development and application of neuroanalytical techniques to study neurodegenerative diseases.